Acoustic Model of the Remnant Bubble Cloud from Underwater Explosion

Alexei Kouzoubov (1), John Castano (2), Carlos Godoy (2) and Mark Hyman (3)

(1) Defence Science and Technology Organisation, Edinburgh, SA, Australia
(2) Naval Undersea Warfare Center, Newport, RI, USA
(3) Naval Surface Warfare Center, Panama City, FL, USA

ABSTRACT

A model of formation, development, and acoustic properties of the bubble cloud resulting from an underwater explosion is presented. The model includes several parts: explosion globe dynamics, initial break-up of the explosion globe, turbulence created by the explosion globe fragmentation, and further break-up of the bubbles by the turbulence. The time history of the bubble cloud properties is calculated under the assumption of the cloud being a collection of non-interacting bubbles. Model results are compared with the available experimental data.

INTRODUCTION

It is of interest for some defence applications to understand the dynamics and to model the acoustic properties of the bubble cloud remnant of the underwater explosion. There are not many papers published on the subject. We are only aware of one (Holt&Culver, 2011), in which the remnant bubble cloud is investigated experimentally by acoustic method. To the best of our knowledge, there were no attempts to develop a theoretical model of the remnant bubble cloud formation and dynamics. The present document reports the development of such a model. We apply a physics-based approach and avoid complex and computationally demanding numerical simulations. Such an approach will undoubtedly require certain approximations and the introduction of some empirical parameters into the model. These will have to be adjusted from the comparison with the existing or future experimental data or high-fidelity numerical simulations. We, however, are not aware of any such accurate numerical simulations of this problem. Taking into account the complexity of the phenomenon, it is unlikely that such simulations could be performed in the near future.

MODEL OUTLINE

As a result of an underwater explosion (UNDEX), a gas globe is formed, which experiences several expansions and contractions during short time after the detonation. We will use the term "globe" for the initial gas bubble formed by the underwater explosion to distinguish it from the bubbles as product of the initial globe disintegration. During these oscillations the explosion globe rises in water, especially quickly during contraction phases when the drag force is lower. After two to three oscillations the large explosion bubble disintegrates into a large number of smaller bubbles, which then rise towards the surface of water with various speeds depending on their size. The purpose of this model is to estimate the bubble size distribution, the bubble spatial distribution and the dynamics of their rise. The acoustic properties of the remnant bubble cloud can be easily derived from the known bubble size distribution.

The steps of the currently suggested model are summarised below. The references to specific model elements will be given in the corresponding sections of the paper.

- The oscillations and rise of the explosion globe are based on the models available in the literature, with slight modifications, of spherical bubble shape dynamics and motion. There are more sophisticated numerical models describing the UNDEX globe oscillation and rise, but for the purpose of this research the current, computationally efficient approach will suffice.

- It is assumed that at the third minimum of the UNDEX globe oscillation, it disintegrates into smaller bubbles. The size distribution of the fragments is estimated from the growth rate of the modes of the Rayleigh-Taylor instability for spherical cavity. It is assumed that initial pressure of gas in the fragments is the same as in the explosion globe just before the break-up. Then the bubbles expand to bring the internal gas pressure into the balance with the ambient pressure. The resulting bubble cloud size is estimated as being proportional to the total gas volume. The coefficient of proportionality is treated as an empirical parameter in the current model.

- The explosion globe potential energy at the minimum of its radius goes into the kinetic energy of the turbulent spot in the fluid. The time-space distribution of the turbulent kinetic energy is obtained by solving the corresponding equation in approximation of spherical symmetry.

- The bubbles resulting from the initial fragmentation of the explosion globe are further broken-up by turbulence. To describe this, one of the bubble break-up models is used. It should be noted here that all of the bubble break-up models by turbulence are developed in the assumption of small gas volume fraction and isotropic nature of turbulence. In this problem, the gas volume fraction is high and the turbulence is not isotropic. However, in the absence of a better model, one of the existing models is applied with a note of addressing this problem in future. The unsteady equation of the bubble population balance is solved using the time-space distribution of the turbulence obtained in the previous step.

- The rise of the bubbles to the surface is then calculated from the balance of the buoyancy and drag forces. The spatial and size distribution of the gas volume fraction is then used to estimate the acoustical properties of the gas bubble cloud.

OSCILLATIONS AND RISE OF THE EXPLOSION BUBBLE

There exist sophisticated numerical models of the explosion globe rise and oscillations. Here, for the sake of UNDEX remnant bubble cloud model development, we need a relatively simple, computationally efficient estimation of the bubble radius and pressure inside the bubble at the beginning of the explosion bubble break-up. In the current model we base our estimation on a relatively simple equation of a spherical bubble motion and oscillations. Later, these estimations may be obtained from a more sophisticated numerical model.

The models of the oscillations and motion of the explosion bubble, sometimes referred to as globe here to distinguish from the bubbles resulting from the explosion globe fragmentation, date back to 1940s (*Underwater Explosion Research*, 1950; Cole, 1948). The early models were based on the assumption of incompressible flow and did not take into account the energy loss due to pressure wave radiation during the collapse-rebound stage of bubble oscillation. As a result they did not account for the damping of bubble shape oscillations observed in experiments. Recently a model has been published (Geers&Hunter, 2002), which accounts for the wave effect. The model is based on the doubly asymptotic approximation and combines relative simplicity based on the assumption of spherical shape of the explosion globe with the reasonable prediction of the globe oscillation damping. In our model of formation of the UNDEX remnant bubble cloud we employ this model of the explosion bubble oscillations with some modifications. Thus the radius of the spherical explosion globe, R, is described by the following equation:

$$R\ddot{R}f_1 + \frac{3}{2}\dot{R}^2 f_2 + \dot{R}f_3 = \frac{1}{\rho_l} f_4 + \frac{|\mathbf{u}-\mathbf{u}_b|^2}{4} \qquad (1)$$

where ρ_g, ρ_l is the density of gas inside the bubble and surrounding liquid, respectively, c_g, c_l is the speed of sound in gas and liquid, p_∞ is the ambient pressure of surrounding fluid, p_{g0} is the initial gas pressure inside the bubble. We do not reproduce here the functions f_1, f_2, f_3 and f_4 referring to Geers&Hunter (2002) (Equations 32 and 33). The second term on the right-hand side of the equation (1) is due to the added pressure on the bubble surface resulting from the bubble motion (Hsiao et al., 2003). We include this term in addition to the model provided by Geers&Hunter (2002).

Initial conditions for equation (1) are obtained from combination of similitude relation for the far-field shock-wave pressure profiles and the volume acceleration model (Geers&Hunter, 2002). The bubble translation model described in the same paper does not, however, provide a satisfactory result unless an artificial drag coefficient is introduced. Therefore, we have chosen to use the following equation often applied to modelling of bubble motion (Hsiao&Pauley, 1999):

$$\left(\rho_g + \frac{1}{2}\rho_l\right)\frac{d\mathbf{u}_b}{dt} = \left(\rho_g - \rho_l\right)\mathbf{g} + \frac{3}{8}\rho_l C_D \frac{1}{R}(\mathbf{u}-\mathbf{u}_b)|\mathbf{u}-\mathbf{u}_b| + \frac{3}{2R}\rho_l(\mathbf{u}-\mathbf{u}_b)\frac{dR}{dt}. \qquad (2)$$

In this equation $\mathbf{u}_b$ is the velocity of the bubble, $\mathbf{u}$ is the velocity of the surrounding fluid, $\mathbf{g}$ is the acceleration due to gravity, and C_D is the drag coefficient. Here we use the Grace Drag model (Clift et al., 1978; *ANSYS CFX-Solver*, 2010), which accounts for wide range of bubble Reynolds number and various regimes of bubble deformation.

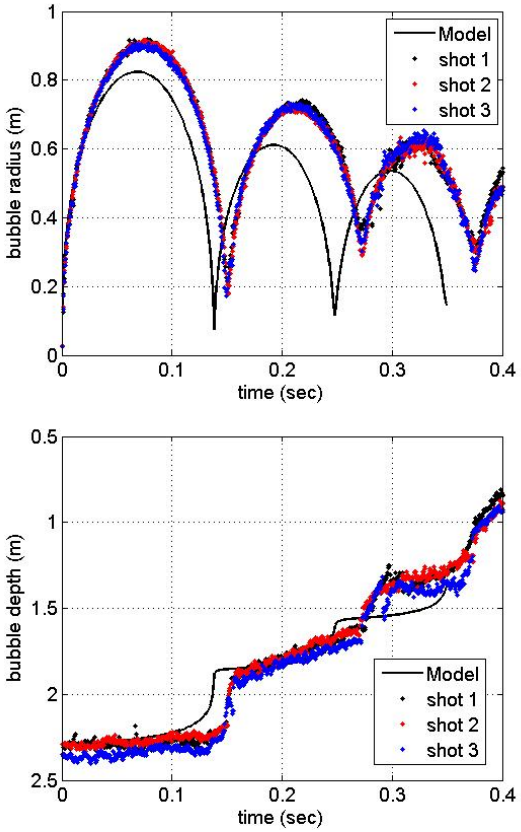

Figure 1. Explosion globe radius (top plot) and depth (bottom plot).

Here we will consider an example from the laboratory UNDEX experiment conducted at the Carderock Division of the Naval Surface Warfare Center (Harris et al., 2010). In this experiment 0.23 kg (0.5 lb) of pentolite explosive was detonated at 2.29 m (7.5 feet) of depth. The result of applying the above model to this case is presented in Figure 1 together with the experimental results obtained by processing video taken during the experiment. It should be noted here that the above mentioned report does not specify the exact composition of explosive used in the experiment and there are several versions of the explosive called pentolite. In the model realisation we used the physical parameters for pentolite available in the literature. More accurate data on the physical properties of the specific explosive used in the test may improve the agreement between the model and experimental data. Nevertheless, the current model gives much better agreement than the usual bubble oscillation models which do not take into account the energy loss due to shock wave.

EXPLOSION GLOBE FRAGMENTATION

We assume that the explosion globe break-up occurs at the third minimum as a result of instability of the bubble spherical shape. It is a simplification because in reality the fragmentation of the explosion globe occurs in steps at the second, third, and even fourth minimum of the breathing modes, which could be seen from the video sequence (Harris et al.,

2010). However we believe that compressing this process into one single act of fragmentation is a reasonable assumption which significantly simplifies the model. The model improvement in this respect may be addressed in future work.

Just before the explosion globe break-up its radius is R_0^* and the gas pressure inside the bubble p_{g0}^*. In the current model we obtain these values from the solution of equations in the previous section. Alternatively, they can be obtained from a more accurate numerical model of underwater explosion.

We estimate initial bubble size distribution from the modes of the Rayleigh-Taylor instability for the spherical bubble. The growth rate of the non-spherical distortions on the bubble surface is proportional to the following value (Brennen, 2002):

$$f(m) = (m-1)\left[\Gamma - (m+1)(m+2)\right] \tag{3}$$

where $\Gamma = \rho R^2 \ddot{R}/\sigma$ and m is the order of a spherical harmonic distortion. We postulate that each mode m leads to bubbles of size $r_m = R_0^*/m$ in the daughter bubble cloud and that the number of bubbles of this size is proportional to the function $f(m)$:

$$\begin{aligned} n_m &= A(m-1)\left[\Gamma_0^* - (m+1)(m+2)\right] \\ &= A\left(\frac{R_0^*}{r_m} - 1\right)\left[\Gamma_0^* - \left(\frac{R_0^*}{r_m}+1\right)\left(\frac{R_0^*}{r_m}+2\right)\right] \end{aligned} \tag{4}$$

where Γ_0^* is the value of Γ at $R = R_0^*$. The normalisation coefficient A is determined from the balance of the gas volume:

$$\sum_m n_m \Delta r_m r_m^3 = \left(R_0^*\right)^3 \tag{5}$$

We assume that straight after the break-up the gas in the daughter bubbles has the same pressure, p_{g0}^*, as the explosion bubble just before break-up. Then the bubbles expand to reach the balance with the pressure in the surrounding fluid. We assume here that during globe break-up the gas temperature rapidly adjusts to the temperature of water and subsequent expansion of break-up products is isothermal. The new bubble size can be obtained from the following equation:

$$p_1 V_1 = p_2 V_2, \tag{6}$$

where $p_1 = p_{g0}^*$ and $p_2 = p_a + \rho g h_b + 2\sigma/\tilde{r}_m$, h_b being the depth of the bubble, and p_a the atmospheric pressure. This results in the following cubic equation for the new bubble radius, $\tilde{r}_m$:

$$\tilde{r}_m^3 + \frac{2\sigma}{p_a + \rho g h_b}\tilde{r}_m^2 - \frac{p_{g0}^*}{p_a + \rho g h_b} r_m^3 = 0. \tag{7}$$

If the surface tension can be neglected, this equation simplifies significantly:

$$\tilde{r}_m = r_m \left(\frac{p_{g0}^*}{p_a + \rho g h_b}\right)^{1/3}, \tag{8}$$

however, with the modern computers solving the cubic equation does not affect the overall computation time noticeably. The new bubble size distribution is calculated as:

$$\tilde{n}_m = n_m \frac{\Delta r_m}{\Delta \tilde{r}_m}, \tag{9}$$

and the new total volume of the bubbles in the cloud is:

$$\tilde{V} = \left(\frac{4\pi}{3}\right)\sum_m \tilde{n}_m \Delta\tilde{r}_m \tilde{r}_m^3. \tag{10}$$

The radius of the bubble cloud can be estimated as follows:

$$\tilde{R} = \alpha_C \left(\frac{3\tilde{V}}{4\pi}\right)^{1/3}. \tag{11}$$

Currently we consider α_C as an empirical parameter. Obviously, $\alpha_C > 1$.

Continuing with the example from the previous section and assuming $\alpha_C = 1.5$, we obtain the bubble size distribution shown in Figure 2.

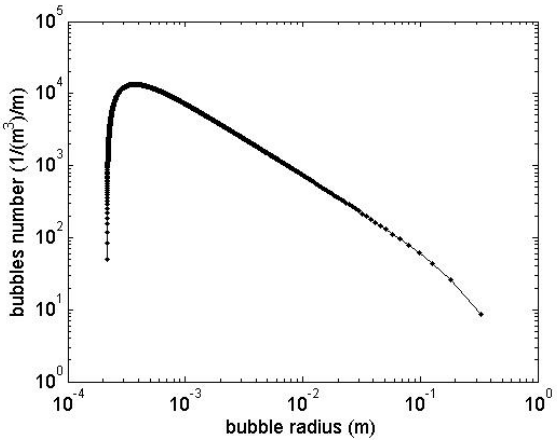

Figure 2. Estimated bubble size distribution after the initial break-up of the explosion bubble.

TURBULENCE RESULTING FROM EXPLOSION BUBBLE BREAK-UP

We assume that almost all potential energy of the explosion bubble before break-up transfers into the turbulent kinetic energy, which then gradually decays due to dissipation, breaking further the bubbles in the remnant bubble cloud. The potential energy of the compressed explosion globe is computed as the work performed against external pressure during globe adiabatic expansion from the compressed state to the state of equilibrium with the external pressure (Cole, 1948):

$$\Pi = 4\pi \int_{R_0}^{R_1} \left[p(r) - P_\infty\right] r^2 dr. \tag{12}$$

Here $P_\infty = p_a + \rho g h_b$ is the ambient pressure at the bubble depth, h_b. During adiabatic expansion the pressure inside the bubble is changing according to the following equation:

$$p(r) = P_0\left(\frac{R_0}{r}\right)^{3\gamma}. \quad (13)$$

Obviously, R_1 is obtained from equation (13) when $p(R_1) = P_\infty$. Integration of (12) will give the following equation for the bubble potential energy:

$$\Pi = \frac{4\pi}{3}R_0^3\left\{\frac{P_0}{1-\gamma}\left[\left(\frac{P_0}{P_\infty}\right)^{\frac{1-\gamma}{\gamma}} - 1\right] - P_\infty\left[\left(\frac{P_0}{P_\infty}\right)^{\frac{1}{\gamma}} - 1\right]\right\} \quad (14)$$

When bubble breaks its potential energy mainly goes into the kinetic energy of the fluid creating a turbulent spot with the total kinetic energy

$$K_0 = \beta_K \Pi, \quad (15)$$

where $\beta_K < 1$ accounts for energy loss due to change in surface energy and acoustic radiation. In the current research we neglect these losses and assume $\beta_K \approx 1$. We assume also that the initial radius of the turbulent spot coincides with the radius of the bubble cloud, $\tilde{R}$. Thus the initial condition for the turbulent kinetic energy per unit mass is:

$$k = \begin{cases} k_0, & r \le \tilde{R} \\ 0, & r > \tilde{R} \end{cases} \quad (16)$$

where $k_0 = \dfrac{3K_0}{4\pi\rho\left(1-\alpha_C^{-3}\right)\tilde{R}^3}$. The decay of the turbulent kinetic energy is described by the following equation (Wilcox, 1994):

$$\frac{\partial k}{\partial t} = -C_\mu\frac{k^{3/2}}{l} + \frac{1}{r^2}\frac{\partial}{\partial r}\left[\frac{\sqrt{k}l}{\sigma_k}r^2\frac{\partial k}{\partial r}\right], \quad (17)$$

For the turbulent parameters in this equation we use the following standard values: $C_\mu = 0.09$, $\sigma_k = 1$, $l = 2\tilde{R}$. Equation (17) is solved numerically using the Crank-Nicolson finite difference method. The dissipation rate of the turbulent kinetic energy, which is used further in the model of the bubble break-up, is calculated according to the following equation:

$$\varepsilon = C_\mu\frac{k^{3/2}}{l} \quad (18)$$

Continuing with the example, Figure 3 shows the decay of the turbulent kinetic energy at the centre of the turbulent spot obtained from the numerical solution of equation (17).

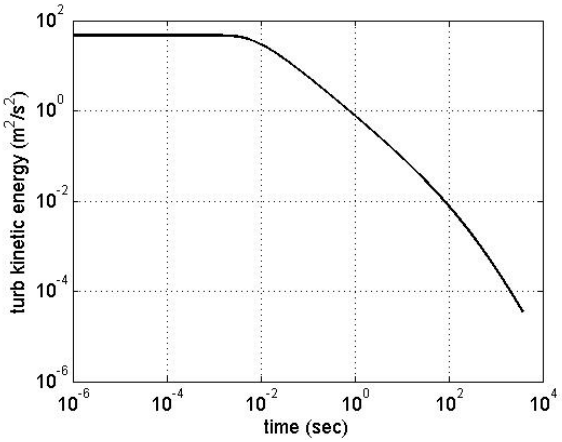

Figure 3. Decay of the turbulent kinetic energy at the centre of the turbulent spot.

FURTHER BUBBLE BREAK-UP BY TURBULENCE

The change of the bubble size distribution, n, due to bubble break-up by turbulence is described by the following equation (Lasheras et al., 2002):

$$\frac{\partial n}{\partial t} = \int_D^\infty m(D_0)f(D,D_0)g(D_0)n(D_0)dD_0 - g(D)n. \quad (19)$$

The first term on the right-hand side of this equation describes the birth rate of bubbles of diameter D; the second term is the death rate of bubbles of this size. In this equation, $g(D)$ is the break-up frequency, $f(D,D_0)$ is the probability density function of the daughter bubbles resulting from the break-up of the mother bubble of size D_0, $m(D_0)$ is the average number of daughter bubbles per one break-up event. Here we use the break-up frequency and daughter bubbles probability density function from (Martinez-Bazan et al., 1999a, 1999b):

$$g(\varepsilon, D_0) = K_g D_0^{-1}\sqrt{\beta(\varepsilon D_0)^{2/3} - 12\frac{\sigma}{\rho D_0}}, \quad (20)$$

$$f(D,D_0) = B\left[\frac{1}{2}\rho\beta(\varepsilon D)^{2/3} - \frac{6\sigma}{D_0}\right] \times\left[\frac{1}{2}\rho\beta(\varepsilon D_2)^{2/3} - \frac{6\sigma}{D_0}\right] \quad (21)$$

In the above equations ε is the dissipation rate of the turbulent kinetic energy, K_g and β are empirical constants, $D_2 = \left(1 - D^3\right)^{1/3}$ is the size of the second daughter bubble, and B is the normalisation factor. The following values for the empirical constants, $K_g \approx 0.25$ and $\beta = 8.2$, are suggested by Martinez-Bazan et al. (1999a, 1999b).

Applying the turbulent kinetic energy obtained in the previous section to the bubble cloud with the initial bubble size distribution from Figure 2 we obtain the final bubble size distribution in the bubble cloud shown in Figure 4.

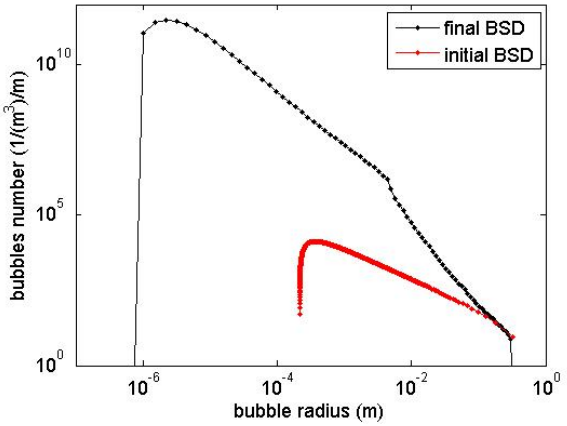

Figure 4. Final bubble size distribution after break-up by turbulence.

RISE OF THE BUBBLE CLOUD

Dissipation of the turbulent kinetic energy in the turbulent spot caused by initial break-up of the explosion bubble occurs relatively quickly. Therefore, we assume that in this time small bubbles in the bubble cloud do not move significantly from their initial positions. Therefore, we assume that the rise of the bubble cloud starts after the bubble break-up by turbulence is finished. Such an approximation simplifies the problem considerably without, we believe, significant loss of accuracy. Another simplifying assumption we make is that the bubbles rise at their terminal velocity, U, obtained from the balance of buoyancy and drag force:

$$(\rho_l - \rho_g)V_b g = \frac{1}{2}\rho_l C_D U^2 A_b \qquad (22)$$

Here ρ_b is the density of the gas inside the bubble, $V_b = \frac{4}{3}\pi R^3$ is the bubble volume, C_D is the drag coefficient, and $A_b = \pi R^2$ is the bubble projected area. Here again we use the Grace Drag model described above.

For each size in the bubble size distribution we calculate the bubble depth, $h_b(t)$, as a function of time from the following kinematic equation:

$$\frac{dh_b}{dt} = -U(h_b)\cdot \qquad (23)$$

The equation (22) and (23) are solved numerically. In this solution we take into account the change in the bubble volume, and as a result all other bubble parameters, due to changing pressure of the ambient fluid.

Under the above assumptions all bubble trajectories will be vertical lines with the different variation of bubble depth with time depending on the initial bubble size. Mathematically, we can describe the bubble trajectories by the following equations in the coordinate system (x, y, z) with x, y being horizontal coordinates and z vertical:

$$(x_b, y_b, z_b) = (x_0, y_0, z(z_0, r_m^{(0)}, t))\cdot \qquad (24)$$

While computing bubble trajectories for different bubble sizes we assume that they all originate from the centre of the bubble cloud. The trajectories are then simply translated into a relevant position of their starting point in the bubble cloud for subsequent computation of the volume fraction in the rising bubble cloud. In this assumption equation (24) can be written in the following form:

$$(x_b, y_b, z_b) = (x_0, y_0, z_0 + f_z(z_C, r_m^{(0)}, t)), \qquad (25)$$

where z_C is the z-coordinate of the initial bubble cloud centre.

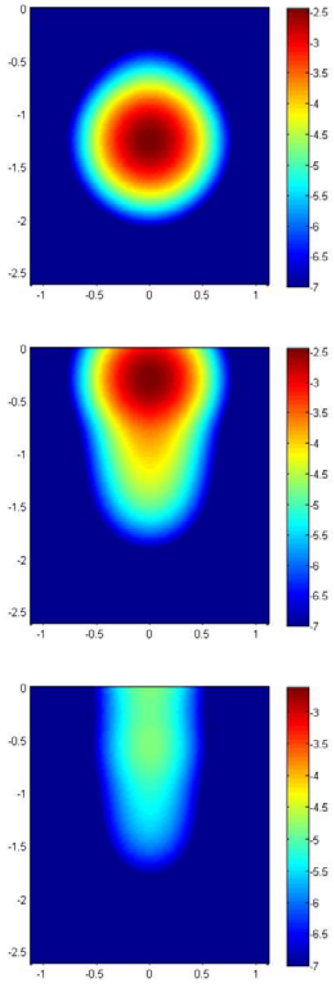

Figure 5. Logarithm of volume fraction at different time moments (from top down): 1, 5, and 20 sec from start of bubble cloud rise.

To calculate the volume fraction in the rising bubble cloud we divide the initial bubble cloud into many volume elements and originate bubble trajectories for all bubble sizes from each volume element. Each bubble trajectory thus associated with a certain gas volume. Obviously, for smooth solution a sufficient number of volume elements are required. In this example we use 100x100x100 volume elements for initial volume subdivision. Also a sufficient number of bubble size groups are neded to obtain a smooth solution along the vertical coordinate. In this example 20 size groups are used. The spatial region above the initial bubble cloud is divided into volume elements as well and from analysis of interjections of bubble trajectories with these volume elements the volume fraction of the bubble cloud at a certain time is calculated. Figure 5 shows an example of the volume fraction in the rising bubble cloud at the different time moments.

Here we should note that for calculation of the volume fraction and acoustical properties of the bubble cloud we do not use the whole final bubble size distribution (Figure 4). Some of the bubbles in this distribution are still large and will rise to the surface very quickly. In this research we are interested in the properties of the bubble cloud at the relatively long time after the detonation, on the order of several minutes. This means a bubble cloud consisting of small bubbles. Therefore, in our model we only consider the part of the final bubble size distribution with bubbles less than a certain size. In the example here we used the bubble diameter of 5 mm as the cut-off bubble size.

Once the volume fraction of the bubble cloud is known for the different size bins, the backscattering cross section per unit volume S_{bs} and the spatial attenuation rate α_b due to bubbles are given by the following equations (Medwin&Clay, 1998):

$$S_{bs} = \sum_{i=1}^{N} n_i \Delta\sigma_s(r_i, f), \tag{25}$$

$$\alpha_b = 4.34 S_e = 4.34 \sum_{i=1}^{N} \sigma_e(r_i, f) n_i, \tag{26}$$

where S_e is the extinction cross section per unit volume. The differential scattering cross section of a single bubble

$$\Delta\sigma_s(r_i, f) = \frac{r_i^2}{\left[(f_R / f)^2 - 1\right]^2 + \delta^2} \tag{27}$$

and the extinction cross section of a single bubble

$$\sigma_e(r_i, f) = \frac{4\pi r_i^2 (\delta / \delta_r)}{\left[(f_R / f)^2 - 1\right]^2 + \delta^2}, \tag{28}$$

where the total damping constant

$$\delta = \delta_r + \delta_t + \delta_v \tag{29}$$

is the sum of the reradiation term δ_r, the thermal damping term δ_t, and the viscous damping term δ_v. The damping terms and the resonance frequency, f_R, depend on the physical properties of the bubble gas and the ambient fluid as well as bubble depth. The corresponding equations are given in section 8.2 of Medwin&Clay (1998) and we do not reproduce them here.

Example of the backscattering cross-section per unit volume is shown in Figure 6.

To compare the model with available experimental data (Harris et al., 2010), we compute the mean backscattering cross-section per unit volume in a horizontal slice located at the depth of 0.9 m (three feet), or 1.37 m (4.5 feet) above the point of detonation. In the experiment the acoustic measurements were taken at this horizontal slice with Reson 7125 multibeam sonar. Example of sonar raw data is shown in Figure 7. The light coloured spot in the sonar data indicates the cross-section of the bubble cloud rising from the point of detonation.

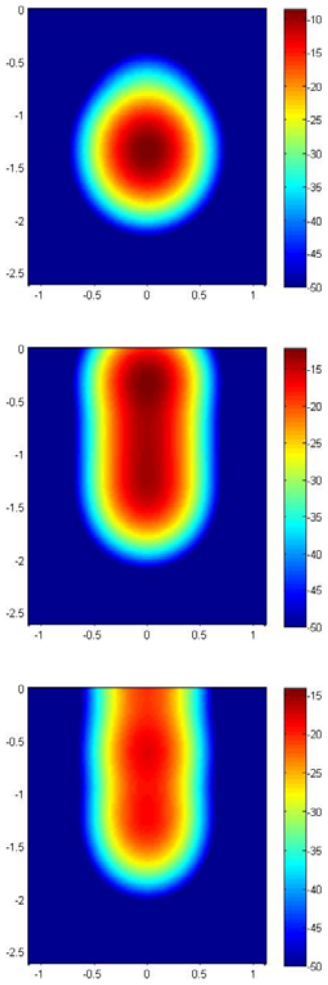

Figure 6. Backscattering cross-section per unit volume at different time moments (from top down): 1, 5, and 20 sec from start of bubble cloud rise.

The backscattering cross-section per unit volume is computed from the raw sonar data, S, as follows:

$$S_V = 20\log_{10} S - G + C - SL + TL - 10\log_{10} V, \tag{30}$$

where SL is the sonar source level in dB, $TL = 2\alpha R + 40\log_{10} R$ is the two-way transmission loss, C is the sonar calibration factor, V is the insonified volume, and $G = G_V + G_C = 2\alpha_0 R + 2\beta\log_{10} R + G_C$ is the sonar gain, consisting of variable and constant parts. From sonar data taken in the air it can be concluded that with high degree of accuracy $\beta \approx 20$. Unfortunately, the sonar was not calibrated for this experiment and the calibration constant, C, is unknown. Here we attempted to calibrate sonar using data on the gas volume fraction and bubble size distribution for the bubble maker, which was also used in the UNDEX experiment (Harris et al., 2010). The sonar data from the bubble maker jet was obtained by the same sonar. On the other hand, the data on the gas volume fraction and the bubble size distribution in the bubble maker jet was acquired in a different laboratory experiment using different measurement techniques by Dynaflow, Inc. Comparing the volume fraction data obtained from the sonar data with the data provided by Dynaflow we calculated the calibration factor. The calculation of the calibration factor was performed in five different locations of the bubble maker jet. The difference between

maximum and minimum values of the calibration factor was 18 dB. There are many factors which can contribute to the uncertainty in the value of the calibration factor with such a non-traditional approach to calibration. The most important among them is turbulent fluctuations of the bubble maker jet. Other factors include inaccuracy in the measurement of the volume fraction and the bubble size distribution.

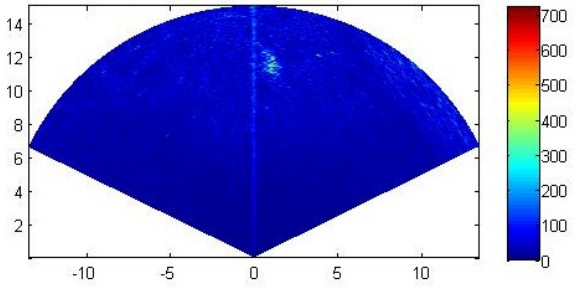

Figure 7. Example of the raw sonar data.

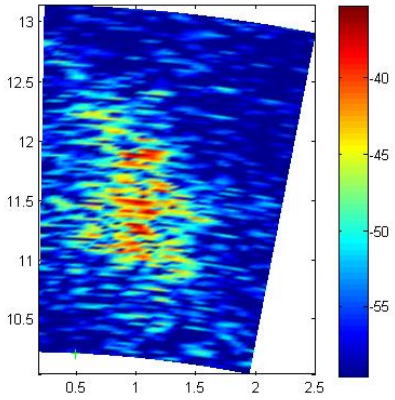

Figure 8. Backscattering cross-section per unit volume calculated from sonar data in a horizontal slice through the bubble cloud.

Using thus obtained calibration factor we processed a sequence of sonar pings in a horizontal slice through the bubble cloud. Example of the backscattering cross-section obtained from the processing of the sonar data, zoomed onto the bubble cloud is shown in Figure 8.

The black curve in Figure 9 shows the mean backscattering cross-section in the horizontal slice of the bubble cloud obtained from processing 800 pings. The error bars on this curve indicate the uncertainty in the calibration factor. The red curve in this figure is obtained from the model.

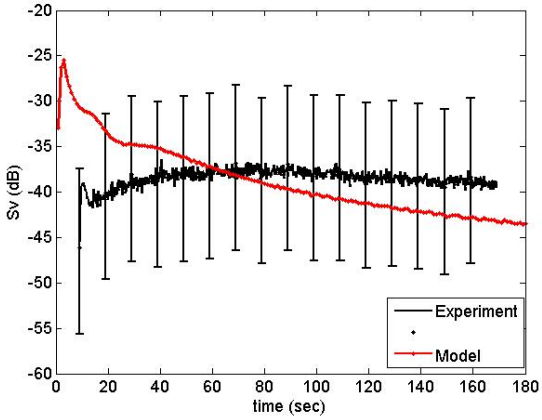

Figure 9. Backscattering cross-section at the horizontal slice of the rising bubble cloud. Depth of the slice location is 3 feet.

CONCLUSION

In this paper we have described the development of the model of formation, dynamics and acoustic properties of the bubble cloud resulting from an underwater explosion. The overall model consists of several sub-models for different steps of the bubble cloud formation and dynamics. These steps include initial explosion globe oscillation and rise, its fragmentation into the smaller bubbles and further break-up of latter by the turbulence created by the explosion globe break-up. The time history of the bubble cloud volume fraction and its acoustic properties is calculated under the assumption that the bubbles in the cloud are not interacting with each other neither hydrodynamically nor acoustically. Comparison of the model with a laboratory experiment shows a reasonable agreement. However, the value of such comparison is somewhat diminished by the fact that the sonar used in the laboratory measurement was not properly calibrated, which introduced a large uncertainty in the experimental data. Further model improvement and validation will be addressed in future.

ACKNOWLEDGEMENT

Authors would like to acknowledge Georges Chahine of the Dynaflow, Inc., Baltimore, MD for providing the bubble maker data.

REFERENCES

ANSYS CFX-Solver, Release 13.0: Theory 2010. ANSYS Inc.

Brennen, CE 2002, 'Fission of collapsing cavitation bubbles', *J. Fluid Mech.*, vol. 472, pp. 153-166.

Clift, R, Grace JR, & Weber, ME 1978, *Bubbles, Drops, and Particles*, London, Academic Press.

Cole, RH 1948, *Underwater Explosions*, Princeton University Press, Princeton.

Geers, TL & Hunter, KS 2002, 'An integrated wave-effects model for an underwater explosion bubble', *J. Acoust. Soc. Am.*, vol. 111, pp. 1584-1601.

Harris, G, Hyman, M, Crane, J, Chahine, G, Lewis, W & Castano, J 2010, *UNDEX Perturbation Test Program.*

Quick Look Report, Naval Undersea Warfare Center, Newport.

Holt, FD & Culver, RL 2011, 'Measuring the Bubble Population Resulting from an Underwater Explosion', *Proceedings of the 4th International Conference and Exhibition on Underwater Acoustic Measurements: Technologies & Results*, pp. 963-70.

Hsiao, C-T, Chahine, GL & Liu, HL 2003, 'Scaling Effects on Prediction of Cavitation Inception in a Line Vortex Flow', *ASME J. Fluids Eng.*, vol. 125, pp. 53–60.

Hsiao, C-T & Pauley, LL 1999, 'Study of Tip Vortex Cavitation Inception Using Navier-Stokes Computation and Bubble Dynamics Model', *ASME J. Fluids Eng.*, vol. 121, pp. 198–204.

Lasheras, JC, Eastwood, C, Martinez-Bazan, C & Montanes, JL 2002, 'A review of statistical models for the break-up of an immiscible fluid immersed into a fully developed turbulent flow', *International Journal of Multiphase Flow*, vol. 28, no. 2, pp. 247-78.

Martinez-Bazan, C, Montanes, JL & Lasheras, JC 1999a, 'On the breakup of an air bubble injected into a fully developed turbulent flow. I. Breakup frequency', *Journal of Fluid Mechanics*, vol. 401, pp. 157-82.

Martinez-Bazan, C, Montanes, JL & Lasheras, JC 1999b, 'On the breakup of an air bubble injected into a fully developed turbulent flow. 2. Size PDF of the resulting daughter bubbles', *Journal of Fluid Mechanics*, vol. 401, pp. 183-207.

Medwin, H & Clay, CS 1998, *Fundamentals of acoustical oceanography*, Sydney, Academic Press.

Underwater Explosion Research 1950, Office of Naval Research, Washington, D.C., Vol. 2.

Wilcox, DC 1994, *Turbulence Modeling for CFD*, DCW Industries, Inc., La Canada CA.